Efficient Computation of Antenna Coupling and Fields Within the Near-Field Region

ARTHUR D. YAGHJIAN, MEMBER, IEEE

Abstract—**The theory, techniques, details of the important equations, and description of two computer programs are presented for calculating efficiently the mutual coupling at a single frequency between any two antennas arbitrarily oriented and separated in free space. Both programs emphasize efficiency and generality, and require, basically, the complex electric far field of each antenna, and the Eulerian angles designating the relative orientation of each antenna. Multiple reflections between the antennas are neglected but no other restrictive assumptions are involved. If an electric field component is desired instead of coupling, the receiving antenna is replaced by a virtual antenna with uniform far field. The first computer program computes coupling (or fields) versus transverse displacement of the antennas in a plane normal to their axis of separation. An efficient fast Fourier transform (FFT) program was made possible by "collapsing" the far-field input data and showing that in most cases the spectrum integration need cover only the solid angle mutually subtended by the smallest spheres circumscribing the antennas. Limiting the integration to this solid angle artifically band limits the coupling function, thereby allowing much larger integration increments and reducing run times and storage requirements to a feasible amount for electrically large antennas. The second program is based on a spherical wave representation of the coupling function and rapidly computes coupling (or fields) versus separation distance between the antennas. The spherical wave representation emerged naturally from an intriguing characteristic proven for the mutual coupling function; it, like each rectangular component of electric and magnetic field in free space, satisfies the homogeneous wave equation.**

I. INTRODUCTION

THE THEORY, computer programs, and measurement facilities for efficiently determining the far fields of antennas by measuring the near-field coupling between test and probe antennas have seen extensive development during the past two decades [1]-[16]. However the associated inverse problem of efficiently computing the near-field coupling of two antennas of arbitrary size, orientation, and separation, given the far field of each antenna, has received little attention despite its direct applicability for determining the interference between co-sited antennas, potentially hazardous fields around antennas, and near-field antenna gain-correction factors.

Two major reasons for this lack of attention have been the difficulty in obtaining the complex vectorial far fields that must be supplied to the computer programs, and the difficulty in developing efficient algorithms for performing the required transformations and integrations. The first difficulty is alleviated for antennas measured using near-field techniques which yield complex vectorial far fields routinely [1]-[16], or for antennas that conform to analysis using physical optics, the geometrical theory of diffraction, or similar asymptotic techniques [17]-[21].[1] The second difficulty dictates the primary objective of the present paper: to formulate *general* expressions and associated computer programs that allow the *efficient* determination of near-field mutual coupling between two antennas, given the electric far field of each antenna and neglecting multiple reflections. (These computer programs also compute the electric near field of an arbitrary transmitting antenna by merely inserting a "virtual" receiving antenna with the proper far fields; see footnote 10.)

Emphasis is placed on combining efficiency and generality. General expressions for the coupling of antennas have existed for many years in terms of aperture fields [22], [23], but their numerical evaluation requires an exorbitant amount of computer time for all but electrically small antennas. Moreover the fast Fourier transform (FFT) evaluation of the plane wave, antenna coupling expressions from which much of the theory in this paper is developed, cannot be applied directly over reasonable distances in the near field of electrically large antennas without encountering prohibitive computer times and storage requirements. Asymptotic techniques such as the geometrical theory of diffraction can sometimes be applied directly to estimate efficiently the mutual coupling between antennas with well-defined edges, feeds, and struts, but such techniques are not sufficiently developed to apply to general antennas.

The main body of the paper divides conveniently into two major sections. The first section presents the theory and its practical application for computing the coupling quotient versus relative displacement of two antennas in a transverse plane normal to the axis of separation between them [24], [25], and the second section does the same for coupling versus displacement of two antennas along the separation axis, that is, versus separation distance. The theory for both sections begins with the Kerns plane wave "transmission integral" [1], [2], [4]-[7] expressed in terms of the far fields of the two antennas and generalized to allow for the arbitrary orientation of each antenna. However a different evaluation scheme is required for efficient computation depending on whether coupling values are desired for the antennas displaced transverse to or along the separation axis. In principle the sampling theorem and FFT can be applied directly in both cases, but in practice the required sample spacing (integration increment) is so small for electrically large antennas separated by distances larger than a few antenna diameters that, as mentioned above, computer time and storage become excessive.

For coupling in the transverse plane, the FFT evaluation is salvaged by collapsing the far-field data and showing that, for

Manuscript received September 12, 1980; revised April 3, 1981.

The author is with the Electromagnetic Fields Division, U.S. Department of Commerce, National Bureau of Standards, Boulder, CO 80303.

[1] In cases where accurate far fields are not readily available, estimates of the far fields will yield coupling quotients with accuracies commensurate with the accuracy of the estimated far fields. Sometimes it is believed mistakenly that the errors in the far fields are greatly enhanced as one extrapolates inward to compute near fields or near-field coupling. This is true only if one tries to compute fields or coupling within the reactive zone (typically a wavelength or so) of the antennas.

electrically large antennas, only the far fields within about the solid angle mutually subtended by the smallest spheres circumscribing the two antennas (including feeds, struts, edges, and all other parts of the antennas which radiate, or affect the reception, significantly) are required to obtain reasonably accurate values of coupling. Limiting the integration to approximately this solid angle artificially bandlimits in space the coupling quotient and thus permits larger integration increments as the separation distance increases, in all, reducing computer time to a feasible amount for an arbitrary separation distance. Specifically, the computer program gives coupling values (or fields) on two orthogonal cuts in a designated transverse plane over a distance equal to approximately twice the sum of the diameters of the two antennas. For the sum of the two antenna diameters equal to a hundred wavelengths, the program takes about three minutes to run on a CDC 6600[2] for coupling in the very near field (50 λ separation). Shorter times are required for larger separation distances, e.g., one minute for the same two antennas separated by 200 λ.

For the computation of coupling versus separation distance, a new representation for the transmission integral is formulated. This formulation capitalizes on the interesting result that the coupling quotient, like each rectangular component of electric or magnetic field, and analogous to the mutual power spectrum of partial coherence theory, satisfies the scalar wave equation and thus can be expanded in a series of spherical waves. Because the coefficients of the spherical waves are directly and conveniently determinable from the scalar product of the electric far fields of the two antennas, the coupling (or fields) along an arbitrary radial axis spanning the entire Fresnel region can be computed very rapidly. Specifically, for the sum of the two antenna diameters equal to a hundred wavelengths, this second program computes the coupling quotient (or fields) along a designated radial axis throughout the Fresnel region in less than a minute on a CDC 6600.

The computer storage required by both programs increases as the ratio of the sum of the antenna diameters to wavelength, and computer run time increases as the square of this ratio.

II. COUPLING VERSUS TRANSVERSE DISPLACEMENT OF THE ANTENNAS

The plane-wave scattering matrix (PWSM) description of antennas, introduced by Kerns, forms an ideal theoretical framework on which to base the determination of mutual coupling between two collocated antennas. However, before the existing formulas can be translated into a convenient program which computes coupling efficiently on a transverse plane, three important tasks must be accomplished.

1) The Kerns transmission integral was originally written in terms of the appropriate plane-wave characteristic for each antenna. For our purposes, we want to express the near-field mutual coupling in terms of the far field of each antenna (assuming reciprocal antennas) because usually the far field most conveniently characterizes an antenna and is most efficiently computed from, e.g., a physical optics and/or geometrical theory of diffraction program or from near-field measurements. This task, although straightforward, requires careful attention to the details of definition of the far field, the plane-wave spectrum, and the reciprocity for each antenna.
2) The far fields of each antenna are usually expressed in a Cartesian coordinate system fixed in each antenna. To compute coupling for an arbitrary separation and orientation of two antennas, the coupling formula requires an integration of the scalar product of the two vector far-field patterns in reoriented coordinate systems. Thus, task two consists of expressing the scalar product of the far fields and reoriented coordinates of each antenna in terms of the Eulerian angles from the preferred or fixed coordinates in which the far field of the antenna is given.
3) The third major task is to discover a way to reduce to a reasonable amount the computer time and storage needed to evaluate the final form of the double integrals expressing the mutual coupling versus transverse displacement for electrically large antennas separated by an arbitrary distance.

The details of these three tasks and their accomplishment are described in the following three subsections.

A. The Coupling Quotient in Terms of Far Fields

Consider an arbitrary antenna transmitting with exp $(-i\omega t)$ time dependence located to the left of an arbitrary receiving antenna, as shown in Fig. 1. The antennas may have arbitrary separation and orientation. Assume that only one mode propagates in the waveguide feed to each antenna.[3] The incident and emergent waveguide mode coefficients for the left antenna are labeled a_0 and b_0, respectively, and for the right antenna, a_0' and b_0', respectively. The reflection coefficients of the right (receiving) antenna and its passive termination are denoted by Γ_0' and Γ_L', respectively.

The *coupling quotient* b_0'/a_0 is a measure of how much signal couples into the receiving antenna per unit input into the transmitting antenna. If the same type of waveguide feeds each antenna and the receiving waveguide is terminated in a perfectly matched load, $|b_0'/a_0|^2$ *equals the amount of power coupled to the receiving antenna per unit power incident to the transmitting antenna.* (This power ratio expressed in decibels is commonly referred to as the *insertion loss ratio* or simply *coupling loss*.) Thus b_0'/a_0 is indeed the major parameter of interest in determining, e.g., mutual interference between antennas.

The transmission integral which gives the coupling quotient in terms of the transmitting and receiving plane-wave characteristics of the respective antennas can be found directly from Kerns [2, pp. 87 and 121]:

$$\frac{b_0'}{a_0} = \frac{1}{1-\Gamma_L'\Gamma_0'} \int_{-\infty}^{\infty}\int_{-\infty}^{\infty} s_{02}'(\mathbf{k}) \cdot s_{10}(\mathbf{k}) e^{i\gamma d} e^{i\mathbf{K}\cdot\mathbf{R}}\, d\mathbf{K}, \tag{1}$$

[2] The CPU time for this computer is rated at about 2.5 × 10^6 instructions per second with about 10^5 central memory words available at 60 bit accuracy. The specific computer is identified in this paper to adequately describe the computer program. Such identification does not imply recommendation or endorsement by the National Bureau of Standards (NBS), nor does it imply that the computer identified is necessarily the best available for the purpose.

[3] If more than one mode propagates in one or both of the feeds, this analysis can be applied for each possible transmit-receive pair of modes; and thus the analysis can be applied to "out-of-band" coupling (provided, of course, that the far fields of each antenna are known at the out-of-band frequency).

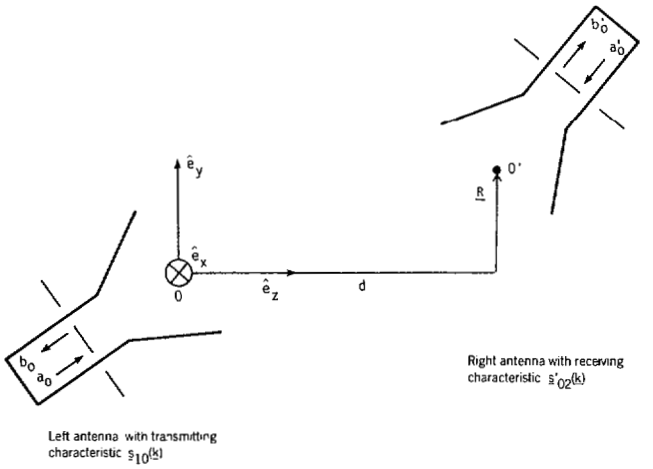

Fig. 1. Schematic of two antennas arbitrarily oriented and separated in free space.

where $\mathbf{s}_{10}(\mathbf{k})$ and $\mathbf{s}'_{02}(\mathbf{k})$ are the vector transmitting and receiving characteristics defined with respect to plane waves traveling in the common $\mathbf{k}$ direction but with phase referenced to the arbitrarily chosen origins 0 and 0′ of the left (transmitting) and right (receiving) antennas, respectively.

As can be seen in Fig. 1, the coordinates $(\mathbf{R}, z = d)$, where $\mathbf{R} = x\hat{e}_x + y\hat{e}_y$, give the position of the origin 0′ fixed in the right antenna with respect to the (x, y, z) coordinate system fixed at 0 in the left antenna. The vector $\mathbf{K} = k_x\hat{e}_x + k_y\hat{e}_y$ is the transverse part of the propagation vector $\mathbf{k} = \mathbf{K} + \gamma\hat{e}_z$ ($k = 2\pi/\lambda$, where λ is the wavelength), and $\gamma = (k^2 - K^2)^{1/2}$ is taken positive real for $K < k$ and positive imaginary for $K > k$. The symbol $d\mathbf{K}$ is shorthand notation for the double differential $dk_x dk_y$. (Although $\mathbf{s}_{10}$ and $\mathbf{s}'_{02}$ are shown as functions of $\mathbf{k}$, they could just as well be written as functions of $\mathbf{K}$ since γ is determined by k_x and k_y.)

Equation (1) is an exact result from Maxwell's equations for two linear antennas operating with $\exp(-i\omega t)$ time dependence in free space for all values of d beyond "encroachment" of the two antennas (defined as the z-separation at which the two antennas overlap with respect to a plane perpendicular to the z-axis and lying between the antennas). Multiple reflections between the antennas are also neglected. In other words, the b_0'/a_0 computed from (1) neglects power that enters the receiver after having been reflected from receiving antenna to transmitting antenna and back one or more times. No other restrictive assumptions are involved. For example, the antennas may be lossy or even nonreciprocal. Of course, (1) cannot be used to evaluate b_0'/a_0 unless the characteristics $\mathbf{s}'_{02}$ and $\mathbf{s}_{10}$ are determined explicitly in terms of commonly measured or computed characteristics of the antennas. Toward this end, both characteristics and (1) are recast next in terms of the electric far fields of the antennas.

As a preliminary to expressing (1) in terms of the far fields of the antennas, assume that the receiving antenna contains no nonreciprocal devices or material so that its receiving functions $\mathbf{s}_{02}'$ are related to its transmitting functions $\mathbf{s}'_{20}$ by the simple reciprocity formula [7],[4]

$$\eta_0'\,\mathbf{s}'_{02}(\mathbf{k}) = \frac{\gamma}{kZ_0}\,\mathbf{s}'_{20}(-\mathbf{k}). \tag{2}$$

[4] If the receiving antenna is nonreciprocal, the formulation must remain in terms of the receiving function $\mathbf{s}'_{02}$.

All quantities in (2) have been defined in the previous section except Z_0, the impedance of free space, and η_0', the characteristic admittance of the propagated mode in the feed waveguide of the right antenna of Fig. 1.

Substitution of $\mathbf{s}'_{02}$ from (2) into (1) gives

$$\frac{b_0'}{a_0} = \frac{(1 - \Gamma_L'\Gamma_0')^{-1}}{kZ_0\eta_0'} \iint_{K<k} \gamma\,\mathbf{s}'_{20}(-\mathbf{k}) \cdot \mathbf{s}_{10}(\mathbf{k}) e^{i\gamma d} e^{i\mathbf{K}\cdot\mathbf{R}}\, d\mathbf{K}. \tag{3}$$

Note that the integral over transverse $\mathbf{K}$ in (3) has been made finite by eliminating the integration over the evanescent part of the spectrum, i.e., the range $K > k$ included in the original infinite integral of (1), thereby leaving only the radiating part of the spectrum. This is permissible for all antennas which are outside each other's reactive field zone, provided the contribution from the integration in (3) near the critical point $K = k$ is negligible, as is usually the case. (Notable exceptions are electrically small antennas, for which the integration near the critical point may contribute significantly for certain orientations of the antennas.) To ascertain in practice that this latter provision is satisfied, the variation in coupling quotient can be observed as the upper limit of integration for K is varied (see Section II-C).

A major advantage of the PWSM technique is that the radiating characteristic of an antenna for $K < k$ is proportional to the vector far field $\mathbf{E}(\mathbf{r})_{r\to\infty}$ of the antenna. Specifically, if $\mathbf{f}(\mathbf{r})$ refers to the normalized complex electric far-field pattern of the left antenna of Fig. 1 measured with respect to the origin 0, i.e.,

$$\mathbf{f}(\mathbf{r}) \equiv \frac{re^{-ikr}}{a_0}\,\mathbf{E}(\mathbf{r})_{r\to\infty}, \tag{4}$$

then the radiating characteristic $\mathbf{s}_{10}(\mathbf{k})$ for $K < k$ is related to the complex far-field pattern by the disarmingly simple proportionality [7],

$$\mathbf{s}_{10}(\mathbf{k}) = \frac{i}{\gamma}\,\mathbf{f}(\mathbf{k}). \tag{5}$$

Although $\mathbf{f}$ is shown as a function of $\mathbf{r}$ in (4), we know that the complex far-field pattern is a function of only the direction of $\mathbf{r}$; and thus $\mathbf{f}(\mathbf{k})$ in (5) is also a function only of the direction of $\mathbf{k}$ which is determined solely by the relative size of k_x and k_y, the integration variables of (3).

Similarly, the radiating characteristics $\mathbf{s}'_{20}$, $K < k$, for the right antenna in Fig. 1 can be written in terms of the normalized complex electric far-field pattern $\mathbf{f}'$ of that antenna:

$$\mathbf{s}'_{20}(-\mathbf{k}), = \frac{i}{\gamma}\,\mathbf{f}'(-\mathbf{k}), \tag{6}$$

where, as in (4), $\mathbf{f}'$ is defined in terms of the electric far field $\mathbf{E}'(\mathbf{r})_{r\to\infty}$ of the right antenna when it is radiating:

$$\mathbf{f}'(\mathbf{r}) \equiv \frac{re^{-ikr}}{a_0'}\,\mathbf{E}'(\mathbf{r})_{r\to\infty}. \tag{7}$$

Substitution of the characteristics from (5) and (6) into (3) produces the coupling quotient for two antennas as a double integral over the scalar product of the complex electric far-

field patterns of the antennas:

$$\frac{b_0'}{a_0} = -\frac{C'}{k} \iint_{K<k} \frac{f'(-\mathbf{k}) \cdot \mathbf{f}(\mathbf{k})}{\gamma} e^{i\gamma d} e^{i\mathbf{K}\cdot\mathbf{R}}\, d\mathbf{K}, \tag{8}$$

where C' is consolidated notation for the "mismatch factor"

$$C' = (1 - \Gamma_L'\Gamma_0')^{-1}/Z_0\eta_0'. \tag{9a}$$

The coupling quotient b_0'/a_0 in (8) is a measure of the signal which is received by the passively terminated antenna on the right side of Fig. 1 when an input mode of unit amplitude is applied to the transmitting antenna on the left. A natural and important consideration is the coupling to the left antenna when the right antenna transmits at the same frequency and the left antenna is terminated in a passive load. Specifically, what is the expression for b_0/a_0' and how is it related to b_0'/a_0 of (8)?

The answer to this question can be obtained immediately by retracing the steps in the derivation of (8) but with the left antenna in Fig. 1 receiving and the right antenna transmitting. This yields an expression for b_0/a_0' very similar to (8). In fact one finds

$$C' \frac{b_0}{a_0'} = C \frac{b_0'}{a_0}, \tag{9b}$$

where the mismatch factor C is defined like C' but for the left antenna. *This means that if the coupling between two reciprocal antennas is measured or computed with one of the antennas transmitting and the other receiving, the coupling, when the roles of transmitting and receiving are reversed, is also known (through (9b)).* A separate measurement or computation need not be done. Use of (9b), of course, requires knowledge of the reflection coefficients and input admittances of each antenna contained in the definitions of C and C'.

Equation (9b) can also be derived directly from the "system two-port" equations describing the two antennas, by applying the Lorentz reciprocity theorem and knowing that multiple reflections between the antennas are being neglected [7]. It can further be proven that if fields scattered by the receiving antenna have a negligible effect on the transmitting antenna, then the available power at the receiving antenna per unit input power to the transmitting antenna is the same when the roles of receiving and transmitting are reversed.

B. Eulerian Angle Transformations Describing the Arbitrary Orientation of the Antennas

From a quick look at (8), it might be concluded that the analysis required to compute the coupling between two antennas is essentially finished. All we need to do is compute or measure the vector far-field patterns of each antenna, take their scalar product, and perform the double integration on a computer.

Unfortunately a major problem, ignored so far, is that the far-field pattern of an antenna is given with respect to a Cartesian coordinate system which is fixed in the antenna and which is not, in general, aligned with the Cartesian system shown in Fig. 1 to which the far-field patterns $\mathbf{f}(\mathbf{k})$ and $\mathbf{f}'(-\mathbf{k})$ in (8) are referenced. Thus, to use (8), it is mandatory that the far-field direction in the coordinate system fixed in each antenna corresponding to a given (k_x, k_y) in (8) be determined explicitly. Moreover, to evaluate the dot product $\mathbf{f}'\cdot\mathbf{f}$, the rectangular components of $\mathbf{f}$ and $\mathbf{f}'$ in the $x - y - z$ system of Fig. 1 must be expressed in terms of the rectangular components of the coordinate systems fixed in the antennas. Fortunately all these necessary transformations can be accomplished by specifying the Eulerian angles required to align the axes fixed in each antenna with the (x, y, z) axes chosen in Fig. 1.

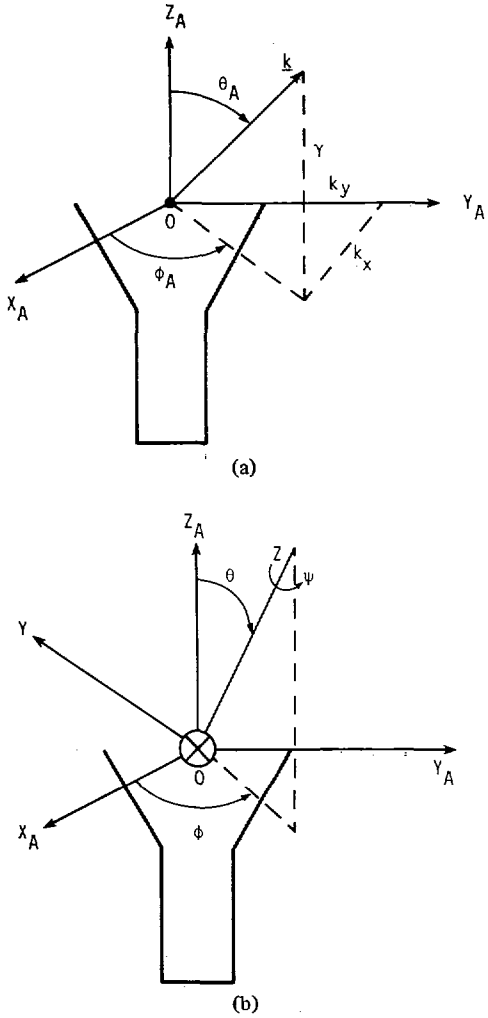

Fig. 2. Definition of coordinates for left antenna of Fig. 1. (a) Coordinate system fixed to the left antenna in which the far field $\mathbf{f}$ is known as function of ϕ_A, θ_A. (b) Eulerian angles (ϕ, θ, ψ) needed to rotate the fixed axes x_A, y_A, z_A to the coupling axes x, y, z of Fig. 1.

Assume the left antenna in Fig. 1 has a fixed coordinate system with rectangular axes $(x_A, y_A, z_A$ centered at 0) in which the normalized electric-far-field pattern is given in terms of the spherical angles ϕ_A and θ_A, as shown in Fig. 2(a). That is, we have at our disposal, obtained from either measurement or computation, the vector far-field pattern $\mathbf{f}(\phi_A, \theta_A)$ as a function of ϕ_A and θ_A. Let (ϕ, θ, ψ) be the Eulerian angles needed to rotate the (x_A, y_A, z_A) axes in line with the (x, y, z) coupling axes of Fig. 1, as specifically shown in Fig. 2(b).

To understand the transformation needed to evaluate (8), note in (8) that $\mathbf{f}$ (and $\mathbf{f}'$) are written as functions of $\mathbf{k} = k_x\hat{e}_x + k_y\hat{e}_y + \gamma\hat{e}_z$ or, in other words, as functions of k_x and k_y, because γ is determined from k_x and k_y. However we are given as known (measured or computed) $\mathbf{f}$ as a function of ϕ_A and θ_A, not k_x and k_y. Consequently, to evaluate (8)

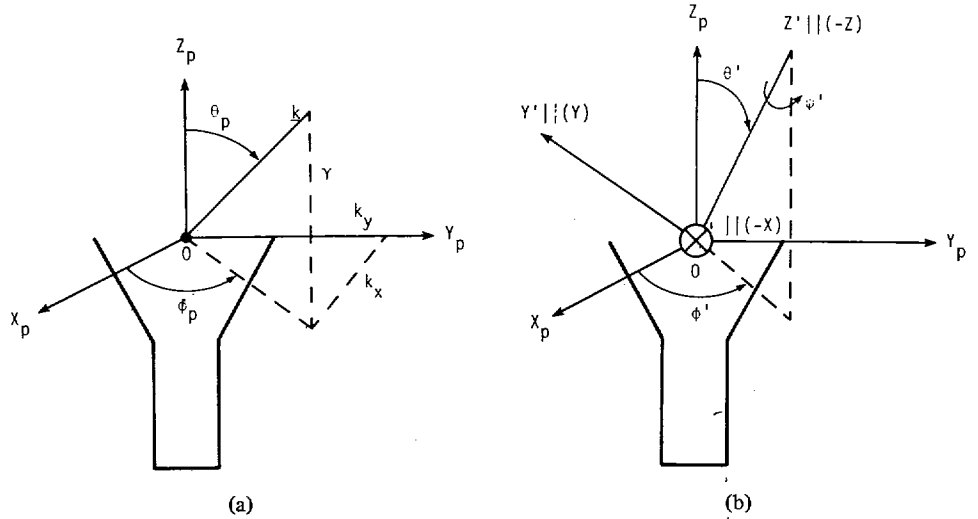

Fig. 3. Definition of coordinates for right antenna of Fig. 1. (a) Coordinate system fixed to right antenna in which the far field $\mathbf{f}'$ is known as function of ϕ_p, θ_p. (b) Eulerian angles (ϕ', θ', ψ') needed to rotate the fixed axes x_p, y_p, z_p to the coupling axes x', y', z', which are in the direction of $(-x)$, (y), $(-z)$ axes of Fig. 1.

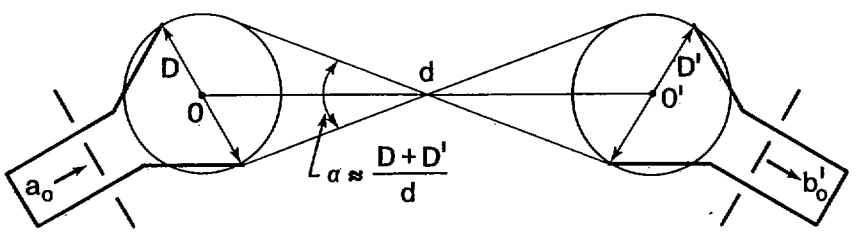

Fig. 4. Physical interpretation for limits of integration. Only that portion of the far fields within about the solid angle α is required to compute coupling quotient for two antennas.

numerically, a transformation is needed that will convert (k_x, k_y) to (ϕ_A, θ_A) under the given Eulerian angles (ϕ, θ, ψ) defining the $x_A - y_A - z_A$ system with respect to the $x - y - z$ system. Similarly, assuming the vector far-field pattern $\mathbf{f}'(\phi_p, \theta_p)$ of the right antenna is given as a function of the spherical angles (ϕ_p, θ_p) measured with respect to axes (x_p, y_p, z_p) fixed in the right antenna, a transformation is needed to convert (k_x, k_y) to (ϕ_p, θ_p) under the given Eulerian angles (ϕ', θ', ψ') defining the $x_p - y_p - z_p$ system with respect to the $x - y - z$ system (see Fig. 3). These Eulerian transformations, which come from a straightforward, rather lengthy, linear transformation found in a number of textbooks [26], are stated in the appendix in the form useful for our purposes of evaluating (8).

C. Limits of Integration, Sample Spacing, and Fast Fourier Transform

In (8) the limits of integration range over the propagating plane waves $K < k$. In this section we show that the range of integration can be reduced further to cover only about the solid angle mutually subtended by the smallest spheres circumscribing the two antennas (see Fig. 4). Thus integration time decreases appreciably with increasing separation distance. Moreover, limiting the range of integration to this solid angle artificially bandlimits the coupling quotient with respect to the transverse displacement $\mathbf{R}$; thereby allowing, through the sampling theorem, larger integration increments and further reduction in computer integration time. In all, computer time is reduced from a prohibitive to an acceptable level.

Rewrite (8) with $\mathbf{R}$ equal to zero and $\mathbf{K}$ expressed in polar coordinates (K, ϕ_0). With the substitution $K = k \sin \beta$, (8) becomes

$$\frac{b_0'}{a_0} = \int_0^{\pi/2} t(\beta) e^{ikd\cos\beta} \sin\beta \, d\beta, \tag{10a}$$

where

$$t(\beta) \equiv -C' \int_0^{2\pi} \mathbf{f}' \cdot \mathbf{f} d\phi_0. \tag{10b}$$

The far-field function $t(\beta)$, if expressed as a Fourier series, contains no higher harmonic frequency than approximately the sum of the largest nonnegligible harmonic frequency of $\mathbf{f}'$ and $\mathbf{f}$. For all but pathologically highly reactive antennas (e.g., highly supergain antennas), the highest possible harmonic frequency in the far field is approximately $kD/2$, where D is the overall dimension of the radiating part of the antenna or 2λ, whichever is larger.[5] (For example, if the left and right

[5] Here we are assuming that the origin to which the far field is referenced is chosen near the physical center of the antenna.

antenna of figure 1 were each an electrically large, circular aperture-type of radiator, D and D' would be their respective diameters; but if one or the other of the antennas were a short dipole, its effective diameter would be set equal to 2λ.) Thus the highest possible harmonic frequency in the function $t(\beta)$ is about $k(D + D')/2$.

As a consequence of this latter result, the integration in (10a) becomes oscillatory when the rate of change with respect to β of $kd \cos \beta$ becomes greater than about twice $k(D + D')/2$. Specifically, the integration in (10a) beyond $\sin \beta_0 = (D + D')/2d$, $d > (D + D')/2$, contributes an amount no larger in magnitude than about $2|t(\beta_0)|/kd$, provided $kd(1 - \cos \beta_0)$ is also greater than about $\pi/4$, i.e., $d < (D + D')^2/\lambda$, the *mutual Rayleigh distance*. Now the function $t(\beta)$ generally decreases appreciably with increasing β because the ϕ_0 integration in (10b) usually encounters more and more fluctuations with ϕ_0 in the far-field scalar product $\mathbf{f}' \cdot \mathbf{f}$ as β becomes larger. Thus, although hypothetical antenna configurations are possible where $t(\beta)$ does not decrease appreciably with increasing β, for most practical computing purposes, the limits of integration in (10a) and (8) need extend only to about $\sin \beta_0 = (D + D')/2d$ or

$$\frac{K_0}{k} = \sin \beta_0 = \frac{(D + D')}{d}, \left(\frac{D + D'}{2} < d < \frac{(D + D')^2}{\lambda} \right). \tag{11a}$$

In practice the computer program increases the K limit of integration beyond K_0 to test whether acceptable convergence has been reached. Equation (11a) has been derived for $R = 0$. Further analysis shows that the result can be made to extend to an $R \approx (D + D')$ by merely doubling the right side of (11a).

Physically (11a) has a very simple interpretation. Referring to Fig. 4, it says that to a good approximation, for ordinary antennas larger than a couple of wavelengths across, only that portion of the far fields within the solid angle mutually subtended by the smallest spheres circumscribing the radiating part of both antennas (including feeds, struts, edges and all other parts of the antennas which radiate or affect the reception significantly) is required to compute the coupling quotient. In other words the far fields can usually be set equal to zero outside about the solid angle α shown in Fig. 4.

As a consequence of this zeroing, the coupling quotient computed from the limited integrations will no longer be equal, even approximately, to the actual coupling quotient for R greater than about $(D + D')$, but will in fact become zero more rapidly beyond $(D + D')$. Specifically a more detailed analysis shows that limiting the range of integration to $K < k(D + D')/d$ also artificially bandlimits the coupling quotient in space to an $R = R_0$ given by

$$R_0 \approx 2(D + D'). \tag{11b}$$

The sampling theorem (see, e.g., [27]) then applied to (8) under this bandlimit converts the integration in (8) to the double summation,

$$\frac{b_0'(\mathbf{R}, d)}{a_0} = -\frac{C'}{k} \Delta k_x \Delta k_y \cdot \sum_{m=-M}^{M} \sum_{l=-L}^{L} \frac{\mathbf{f}'(\phi_p^{lm}, \theta_p^{lm}) \cdot \mathbf{f}(\phi_A^{lm}, \theta_A^{lm})}{\gamma_{lm}} \cdot e^{i\gamma_{lm} e^{di\mathbf{K}_{lm} \cdot \mathbf{R}}}, \tag{12a}$$

with the sample spacing,

$$\frac{\Delta k_x}{k}, \frac{\Delta k_y}{k} \approx \frac{\lambda}{4(D + D')} \tag{12b}$$

and the summation limits

$$L, M \approx \frac{4(D + D')^2}{\lambda d}, \left(\frac{D + D'}{2} < d < \frac{(D + D')^2}{\lambda} \right). \tag{12c}$$

(A simple way to obtain the sample spacing (12b) is to estimate the largest spectral frequency in the integral of (10a) under the bandlimit $\sin \beta \leq (D + D')/d$.) Note that when the separation d approaches the mutual Rayleigh distance $(D + D')^2/\lambda$ only a few points of integration are required, as one might expect from physical intuition because only the near-axis plane waves contribute to the coupling as the far field is approached. The computer program can decrease the values of Δk_x and Δk_y below the values given in (12b) to make certain that small enough integration increments have been used to attain acceptable convergence.

Equation (12a) is amenable to computation by means of the fast Fourier transform (FFT) (see, e.g., [28]). A two-dimensional FFT will compute the double summation in (12a) for a grid of $x - y$ values. However in order to perform all computations for large antennas within the computer central memory core, a one-dimensional FFT program was preferred. This program computes the coupling quotient at a fixed z-separation d on each of two orthogonal cuts ($x = 0$ and $y = 0$) by "collapsing" [29] one summation and performing an FFT on the remaining summation.

D. Numerical Testing of the Program for Coupling Versus Transverse Displacement

In order to build confidence in the computer program which was written to evaluate coupling quotients from (12a), the far fields of two hypothetical antennas were inserted into the program. The hypothetical antennas were linearly polarized (in the x-direction), uniform, circular aperture antennas for which the complex far-field patterns are well-known in terms of simple analytic expressions involving the first-order Bessel function [30]. The radii and operating frequency of the antennas could be chosen arbitrarily in addition to their mutual orientation and separation.

One check performed on the program is displayed graphically in Fig. 5, which shows the coupling quotient for two identical 50 wavelength antennas facing each other in their very near field 50 λ apart. Here the magnitude of the coupling quotient should be very high, actually approaching unity when the antennas are directly aligned, as Fig. 5 confirms. The curve in Fig. 5 is one of two curves which the program produced in a total time of three minutes on a CDC 6600. At a separation distance of 200 λ the program ran in one minute.

A second check of the computer program involves computing the coupling when the antennas are separated by a large enough distance for coupling to take place mainly between the far fields along the direction between the antennas. In Section II-C, this critical distance which we called the "mutual Rayleigh distance" was shown to be approximately $(D + D')^2/\lambda$. In Fig. 6 the coupling between the antennas is computed at this mutual Rayleigh distance for the antennas by two methods—first, by the FFT integration of (12), and then directly from the far-field coupling along the direction of separation.

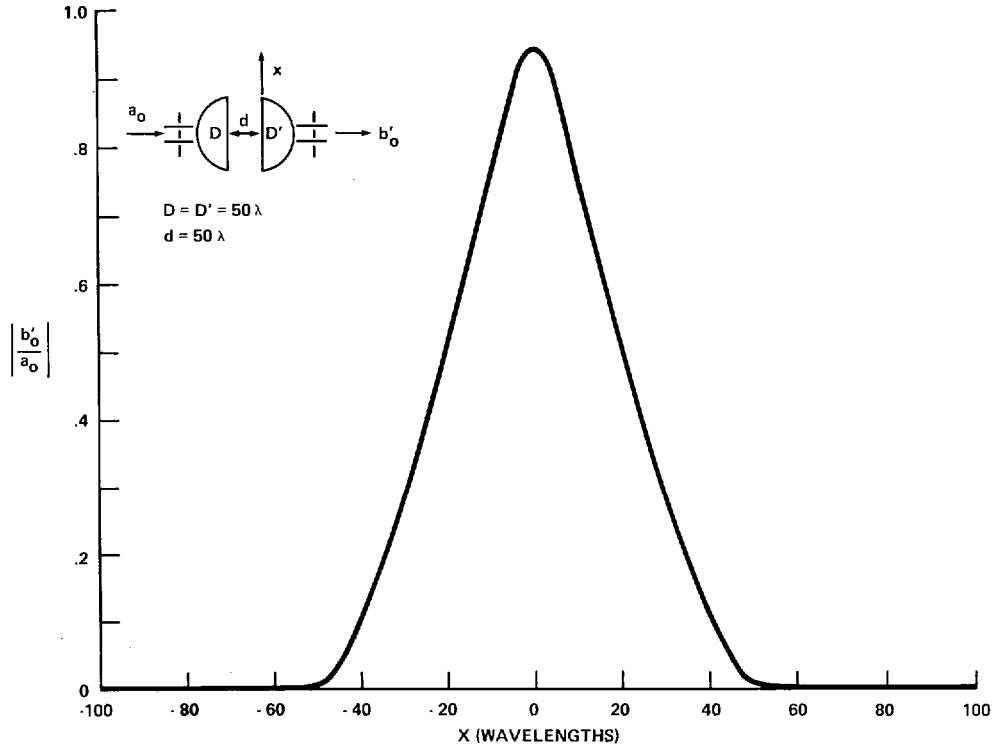

Fig. 5. Hypothetical circular antennas directly facing each other in near field.

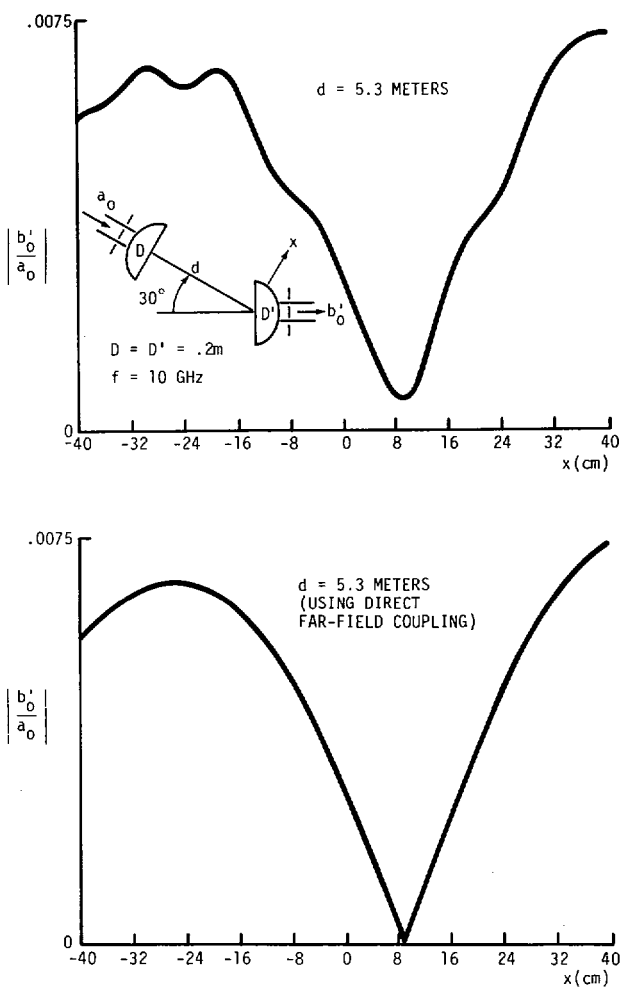

Fig. 6. Coupling of circular antennas computed first using FFT integration, and then directly from far fields along direction of separation.

The agreement between the two results again imbues confidence in the computer program. The ripples in the FFT results occur because the antennas are finitely separated, i.e., are not really in each other's infinite far field.

Finally, Fig. 7 shows a typical coupling curve for the same two antennas as in Fig. 6 skewed in the near field of each other. Further confidence in this first program was also gained through comparing its computed values of coupling with those of the second program which uses a very different computational scheme as described in Section III (note Figs. 5 and 12).

III. COUPLING VERSUS SEPARATION DISTANCE

Section II presented an efficient technique to compute the mutual coupling of two antennas versus relative displacement normal to their z-axis of separation. For many applications, such as determining gain-correction factors for two antennas or computing potentially hazardous fields in the vicinity of antennas, it is desirable to compute coupling loss or fields versus separation distance as well.

At first sight there appears to be a very simple way to do this by applying the FFT to (8) with respect to the exponential $\exp(i\gamma d)$. Specifically, if the differential $d\mathbf{K}$ is written in polar coordinates,

$$d\mathbf{K} = K\, dK d\phi_0 = -\gamma\, d\gamma d\phi_0,$$

(8) becomes for $\mathbf{R} = 0$

$$T = \frac{-b_0'}{C'a_0} = \frac{-b_0}{Ca_0'} = \frac{1}{k}\int_0^{2\pi}\int_0^{k} \mathbf{f}' \cdot \mathbf{f} e^{i\gamma d}\, d\gamma d\phi_0. \tag{13}$$

The ϕ_0 integration can be performed first and the FFT applied to yield the coupling quotient as a function of separation distance d.

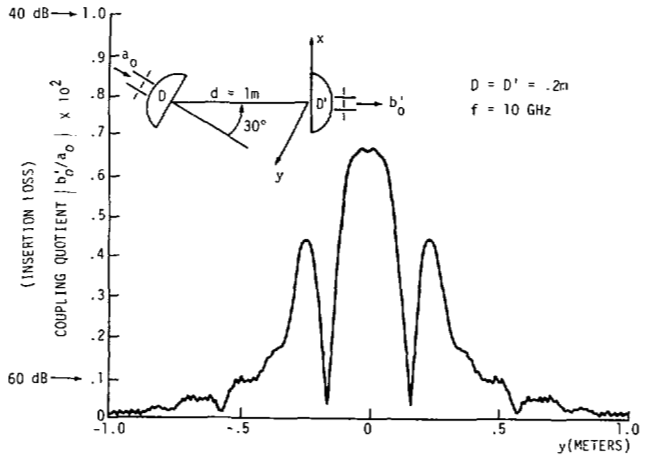

Fig. 7. Typical coupling curve for antennas skewed in their near fields.

The problem with this approach is that the sample spacing in γ required to accurately compute the integral in (13) is so small for reasonably large antennas that computer time is excessive even using the FFT. Moreover, so many sample points are required that in-core computer storage for many commonly used computers also becomes inadequate when applying this FFT approach to large antennas. Thus we are forced to look for an alternative method which will permit efficient computation of coupling versus separation distance for electrically large antennas.

A. Spherical Wave Expansion for the Coupling Quotient

Return to (1) and rewrite a normalized coupling quotient for an arbitrary separation vector $\mathbf{r}$ and propagation vector $\mathbf{k}$ as

$$T(\mathbf{r}) = -Z_0\eta_0' \int_{-\infty}^{\infty}\int_{-\infty}^{\infty} \mathbf{s}_{02}'(\mathbf{k}) \cdot \mathbf{s}_{10}(\mathbf{k}) e^{i\mathbf{k}\cdot\mathbf{r}}\, d\mathbf{K}, \quad (14)$$

where we have let $\mathbf{r} = \mathbf{R} + de_z$, and r equals the distance $00'$. Normally, (14) is defined only for $\mathbf{r}$ and $\mathbf{k}$ in one chosen hemisphere, i.e., one chosen z-axis, and holds for all d outside the encroachment of the two antennas with respect to a plane between the antennas and perpendicular to this z-axis. However the definitions of $\mathbf{s}_{02}'$ and $\mathbf{s}_{10}$ can be continued to all directions of $\mathbf{k}$ and (14) then applies with respect to any z-axis and for all directions of $\mathbf{r}$. (When the direction of z is reversed, Kerns [7] relabels $\mathbf{s}_{02}'$ and $\mathbf{s}_{10}$ by $\mathbf{s}_{01}'$ and $\mathbf{s}_{20}$, respectively. Here, because (14) is simply an intermediate step for proving (16) below, we retain the same labels regardless of the chosen direction of the z-axis.) In review, then, the only assumptions involved in this generalized interpretation of (14) are

1) the two antennas are located in free space and remain in the same relative orientation with respect to Cartesian axes fixed in each antenna as the vector $\mathbf{r}$ from 0 to 0′ varies; that is, the right antenna of Fig. 1 is translated without rotation by the vector $\mathbf{r}$; (recall that 0 and 0′ are the origins to which the characteristics and far fields of the left and right antennas are referenced, respectively);
2) for a given $\mathbf{r}$ there exists some direction of the z-axis for which the separation distance $r = 00'$ is beyond the encroachment distance; and, of course,
3) multiple reflections are neglected.

A sufficient condition for assumption 2) to hold is that the separation distance r remain larger than the sum of the radii of the two spheres centered at 0 and 0′ circumscribing the left and right antenna, respectively. (Actually each sphere need only enclose the significant sources, applied and induced, of its antenna, when radiating.) Letting a and a' denote the radii of the left and right antennas, respectively (see Fig. 8), one can simply state that, neglecting multiple reflections, (14) determines the coupling between any two antennas of fixed relative orientation for all

$$r > r_0 = a + a'. \quad (15)$$

For origins 0 and 0′ near the physical center of the radiating part of their respective antennas, $a \approx D/2$ and $a' \approx D'/2$, where for antennas greater than 2λ across, D and D' were defined in Section II-C as the overall dimension of the radiating part of the left and right antennas.

Equation (14) reveals an intriguing characteristic of the normalized coupling quotient $T(\mathbf{r})$; it, like each rectangular component of electric and magnetic field in free space, satisfies the homogeneous scalar wave equation[6]

$$\nabla^2 T + k^2 T = 0, \quad (16a)$$

for all $\mathbf{r}$ where (14) remains valid, and in particular, for $r > r_0$. In addition, an asymptotic evaluation [7] of (14) as $r \to \infty$ reveals that $T(\mathbf{r})$ satisfies the outgoing radiation condition:

$$T(\mathbf{r})_{r\to\infty} \sim 2\pi ikZ_0\eta_0' \cos\theta_0\, \mathbf{s}_{02}'(\mathbf{r}) \cdot \mathbf{s}_{10}(\mathbf{r}) e^{ikr}/r. \quad (16b)$$

Consequently, $T(\mathbf{r})$ can be expanded uniquely [32] in a series of outgoing scalar spherical wave functions for $r > r_0$ and can be evaluated subsequently by an extremely efficient algorithm.

Since $\exp(-i\omega t)$ time dependence has been assumed, the outgoing spherical waves use spherical Hankel functions of the first kind and $T(\mathbf{r})$ can be written formally as

$$T(\mathbf{r}) = \sum_{n=0}^{\infty}\sum_{m=-n}^{n} B_{nm} h_n^{(1)}(kr) P_n^m(\cos\theta_0) e^{im\phi_0}, \quad r > r_0. \quad (17)$$

The angles (θ_0, ϕ_0) are the spherical coordinate angles of the position vector $\mathbf{r}$ with respect to the (x, y, z) axes fixed in the left antenna. The functions $h_n^{(1)}$ are the spherical Hankel functions of the first kind, P_n^m are the associated Legendre polynomials, and the B_{nm} are the spherical wave coefficients which change for each antenna pair, and for each different relative orientation of the antenna pair.

There are a number of reasons that make (17) especially conducive to the efficient evaluation of coupling versus separation distance. First of all, for coupling along an arbitrary z-axis, θ_0 is zero, $P_n^m(1)$ is nonzero only for $m = 0$ where it equals unity, and (17) reduces to

$$T(d) = \sum_{n=0}^{\infty} B_n h_n^{(1)}(kd), \quad B_n \equiv B_{n0}, d > r_0. \quad (18)$$

We emphasize that (18) is no less general than (17) for coupling quotient versus separation distance because the z-axis can be chosen arbitrarily. Second, the B_{nm} in (17) and thus the B_n

[6] In this respect the mutual coupling function for antennas is analagous to the mutual power spectrum or, equivalently, the spectral density of the mutual coherence function which gives a measure of the partial coherence of radiation between two points in space [39].

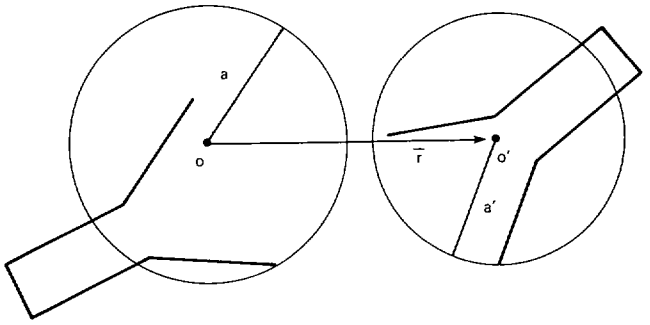

(a) (b)

Fig. 8. Schematic showing radius of each sphere circumscribing the radiating portion of each antenna. (For $r > r_0 = a + a'$ (14) gives correct coupling quotient.) (a) Left antenna. (b) Right antenna.

in (18) are determined efficiently, as will be shown in Section III-B, from an integration of the scalar product of the far fields of the antennas multiplied by the Legendre polynomials. Moreover, for the coupling along a single axis given by (18), we shall show that, within the approximation that the evanescent spectrum is negligible, only the scalar product of far fields in the hemisphere of this axis are required. Third, both the Hankel functions and the Legendre polynomials can be determined by extremely rapid forward recurrence relations which require a meager amount of computer storage. Fourth, because the basic input to the computer program is the same as in Section II, i.e., the scalar product of the far fields of the antennas, all the necessary Eulerian angle transformations are contained in the appendix; and the subroutines required to compute these transformations can be borrowed directly from the previous computer program of Section II.

B. Evaluation of the Spherical Wave Coefficients

To express the B_{nm}, and thus the required B_n of (18), simply in terms of the far fields of the antennas, equate the T in (14) and (17), and let the separation distance r approach infinity. As $r \to \infty$ the spherical Hankel functions in (17) behave as

$$h_n^{(1)}(kr)_{r\to\infty} \sim (-i)^{n+1} e^{ikr}/kr, \tag{19a}$$

and the integral in (14) can be replaced by the first term in its asymptotic series (16b).

For a reciprocal receiving antenna (see footnote 4), one can substitute from (2), (5), and (6) to recast (16b) in terms of the far fields of the antennas:

$$T(\mathbf{r})_{r\to\infty} \sim \frac{-2\pi i}{k} \mathbf{f}'(-\mathbf{r}) \cdot \mathbf{f}(\mathbf{r}) e^{ikr}/r. \tag{19b}$$

With the help of (19a) and (19b), (14) and (17) equate to yield

$$2\pi \mathbf{f}'(-\mathbf{r}) \cdot \mathbf{f}(\mathbf{r}) = \sum_{n=0}^{\infty} \sum_{m=-n}^{n} B_{nm}(-i)^n P_n^m (\cos\theta_0) e^{im\phi_0}. \tag{20}$$

We can multiply (20) by $P_n^m e^{-im\phi_0}$ and use the orthonormality relations [31] for the spherical harmonics to obtain the coefficients B_{nm} in terms of the far fields. Specifically,

$$B_{nm} = \frac{i^n(2n+1)}{2} \frac{(n-m)!}{(n+m)!} \int_0^{\pi} \int_0^{2\pi} \mathbf{f}'(-\mathbf{r}) \cdot \mathbf{f}(\mathbf{r}) P_n^m (\cos\theta_0) e^{-im\phi_0} \sin\theta_0 \, d\phi_0 \, d\theta_0. \tag{21}$$

For $B_n = B_{n0}$ (21) reduces to

$$B_n = \frac{(2n+1)}{2}(i)^n \int_0^{\pi} \int_0^{2\pi} \mathbf{f}' \cdot \mathbf{f} P_n(\cos\theta_0) \sin\theta_0 \, d\phi_0 \, d\theta_0. \tag{22}$$

Given the far fields of the two antennas, (22) can be integrated to determine the B_n, which can in turn be substituted into (18) for the coupling quotient versus separation distance d along an arbitrary z-axis.

There remains the question of how many terms in the summation of (18) are required and what sample spacings are required in the ϕ_0 and θ_0 integrations of (22) for reasonable accuracy. In addition, the scalar product $\mathbf{f}' \cdot \mathbf{f}$ must be written in terms of angles ϕ_0 and θ_0 in order to perform the integrations in (22). However, before dealing with these topics, we will show that only the far fields, i.e., $\mathbf{f}' \cdot \mathbf{f}$, over the surface of one hemisphere is needed to compute coupling in that hemisphere by the method of substituting (22) into (18), provided the evanescent spectrum is negligible.

Equations (14) and (17) are two representations for the same coupling function $T(\mathbf{r})$. Furthermore, (14) determines the coupling quotient in any hemisphere from the far-field scalar product over the surface of that hemisphere, plus the contribution from the evanescent spectrum, regardless of the far fields in the opposite hemisphere. Thus, set the far-field scalar product in the opposite hemisphere equal to zero.[7] Since (17) is an equivalent expression for the coupling quotient, it follows that for coupling computed along the axis in one hemisphere (18) requires the far-field scalar product only over the surface of that hemisphere, assuming that the contribution from the evanescent spectrum is negligible.

Using the scalar product of far fields in one hemisphere only to compute the coefficients B_n from (22) significantly reduces the computer time. In Section II-C, it was further shown that for electrically large antennas only the far fields within about the solid angle mutually subtended by the smallest sphere circumscribing the two antennas usually suffices for reasonably accurate computation of the coupling quotient. Thus if the coupling quotient is required only for separation distances much larger than the sum of the antenna diameters, a solid angular sector much less than a hemisphere could be used and computer run time could be decreased still further. (This latter feature has not been taken full advantage of in the initial program for computing coupling versus separation distance because computer run time was considered small enough without it.)

[7] Although, in principle, analyticity of the spectrum implies that setting the back hemisphere zero can be done only at the expense of changing both the evanescent spectrum and the far-field scalar product in the forward hemisphere, in numerical practice using a fixed number of spherical modes prescribed in Section III-D, these changes contribute negligibly if the contribution from the evanescent spectrum in (14) is negligible.

C. Applicability of Previous Eulerian Angle Transformations

To evaluate the integral for the B_n in (22) for an arbitrarily chosen direction of the z-axis in (18) and arbitrary orientation of the two antennas, the scalar product $\mathbf{f}'(-\mathbf{r})\cdot\mathbf{f}(\mathbf{r})$ must be evaluated as a function θ_0 and ϕ_0 for arbitrary Eulerian angles describing each antenna. Fortunately, the necessary transformations have been described and performed in the appendix (see Figs. 2 and 3).

Specifically the x, y, z components of $\mathbf{r}$ are expressed in terms of θ_0 and ϕ_0 by

$$x = r \sin\theta_0 \cos\phi_0, y = r \sin\theta_0 \sin\phi_0, z = r\cos\theta_0. \quad (23)$$

Once x, y, and z are known, $\mathbf{f}'\cdot\mathbf{f}$ is determined from (A1), (A2), and (A3), given the far fields in the preferred coordinate system of each antenna and the Eulerian angles needed to rotate the axes of the preferred system of the left and right antenna to the (x, y, z) and $((-x), y, (-z))$ axes, respectively.

D. Number of Modes, and Size of Integration and Separation Increments

The infinite summation in (18) must be truncated in order to evaluate it numerically. Thus the approximate value of n at which the B_n evaluated from (22) become negligible must be determined. First consider the case where the major variation in $\mathbf{f}'\cdot\mathbf{f}$ is due to the transmitting antenna's far field $\mathbf{f}$. For example, let $\mathbf{f}' = \hat{e}_{x'}$. Then the coupling given by (18) would be proportional to the x-component of electric field of the transmitting antenna, and the number of modes required beyond a wavelength or so from nonsuper-reactive antennas is approximately $k(a + \lambda)$ [33], [34]. Similarly, if the major variation in $\mathbf{f}'\cdot\mathbf{f}$ were due to the receiving antenna's far field, the number of required modes is approximately $k(a' + \lambda)$. For a general scalar product of two far fields, the maximum variation with θ_0 and ϕ_0 in the scalar product $\mathbf{f}'\cdot\mathbf{f}$ is no greater than approximately the variation of a single antenna of radius $a + a'$. Thus the number N of required modes in the summation of (18) is given approximately by

$$N \approx k(a + a' + \lambda), \quad (24)$$

for nonsuper-reactive antennas separated by more than a wavelength or so, i.e., beyond each other's reactive-field zone. In computational practice, it has been found that the modal coefficients B_n become negligible extremely rapidly as n gets larger than the N given approximately by the formula (24), e.g., see Figs. 11 and 13.

The formula (24) implies that B_n given by the integrals in (22) is bandlimited to $n \approx k(a + a' + \lambda)$, and this can be used to determine the maximum integration increments in ϕ_0 and θ_0 permitted to evaluate the integrals in (22). We evaluate (22) by straightforwardly converting the integrals to summations with equal increments $\Delta\phi_0$ and $\Delta\theta_0$.

Consider the ϕ_0 integration first and define

$$F(\theta_0) = \int_0^{2\pi} \mathbf{f}' \cdot \mathbf{f}(\theta_0, \phi_0) d\phi_0$$

$$\approx \Delta\phi_0 \sum_{l=1}^{L} \mathbf{f}' \cdot \mathbf{f}(\theta_0, \phi_{0l}), \quad (25)$$

where

$$\phi_{0l} = (l-1)\Delta\phi_0 \quad \text{and} \quad \Delta\phi_0 = \frac{2\pi}{L}.$$

The only other information required to evaluate the summation in (25) is the value of L. Since the Fourier series representation of $\mathbf{f}'\cdot\mathbf{f}$ with respect to ϕ_0 is assumed bandlimited by the N given in (24), the sampling theorem [27] tells us that the minimum required value of L is just N.[8]

Equation (25) must be evaluated for each value of θ_0 required to perform the θ_0 integration. From (25) and (22) we can write

$$B_n = \frac{2n+1}{2}(i)^n \Delta\theta_0 \sum_{p=1}^{P} F(\theta_{0p}) \sin\theta_{0p} P_n(\cos\theta_{0p}), \quad (26)$$

where

$$\theta_{0p} = (p-1)\Delta\theta_0 \text{ and } \Delta\theta_0 = \frac{\pi}{P}.$$

Once again we are left only with determining the minimum permissible value of the summation limit P (not to be confused with Legendre polynomials P_n^m and P_n). The minimum value of P can be decided by observing that (26) is required for a maximum n given approximately by N, and that $P_N(\cos\theta_{0p})$ can be written as a sum of exponentials $\exp(\pm in\theta_{0p})$ with $n \leq N$. Thus the sampling theorem [27] again can be applied to show that the minimum required value of P is approximately N.[9] The limits L and P of the summations in (25) and (26) are then given by

$$L \approx P \approx N \approx k(a + a' + \lambda). \quad (27)$$

In the computer program convergence of the ϕ_0 and θ_0 summations can be tested by increasing the values of L and P beyond that given in (27).

Given the electric far field of each of the two antennas, and the Eulerian angles of orientation of each antenna with respect to the rectangular coordinate system to which the far field is referenced, (26) and (25) along with the transformations of the appendix determine the spherical wave coefficients B_n. The coefficients B_n then determine the coupling quotient versus separation distance d from the summation in (18) for $d > r_0 = a + a'$. The spherical Hankel functions in (18) and Legendre polynomials in (26) are computed very efficiently from their recurrence relations [35], and as will be discussed in the concluding remarks, total computer run time and storage become proportional to N^2 and N, respectively, for electrically large antennas.

The size of the increments in separation distance d needed in (18) to resolve the variations in coupling quotient (or

[8] Actually, one can relax this sampling criterion for the $\Delta\phi_0$ increments by redefining a and a' with respect to circumscribing cylinders (rather than spheres) with center lines along the z-axis [13], [14].

[9] The bandwidth N cannot be assumed immediately for the θ_0 exponential integrals because the θ_0 integration ranges only from 0 to π rather than from 0 to 2π. This problem can, however, be overcome by extending the definition (25) of $F(\theta_0)$ to cover the redundant range $\pi \leq \theta_0 \leq 2\pi$ as well, or by arguing that the relatively narrow convolving sinc function introduced by the 0 to π window will broaden the bandwidth negligibly.

fields) throughout the Fresnel region still must be determined. To do this, assume that the variation of coupling quotient with distance d will be no more rapid than the variation of the fields of a single antenna with diameter equal to the sum of the diameters of the two mutually coupled antennas. Fresnel approximations applied to aperture antennas [36] can then be used to show that increments Δd in the separation distance given by

$$\frac{\Delta d}{\lambda} = \frac{1}{2}\left(\frac{d}{D+D'}\right)^2, \qquad d > \frac{D+D'}{2} \tag{28}$$

suffice to resolve the largest variations one could encounter for nonsuper-reactive antennas. (In (28) it is assumed that the separation distance d is measured between origins 0 and 0′ which are physically close, within a diameter or so, to their respective antennas). The total number of points (N_d) spaced according to (28) throughout the near-field region from $(D + D')/2$ to the far field ($\gtrsim (D + D')^2/\lambda$), i.e., throughout the Fresnel region, is given roughly by

$$N_d \approx \frac{k(D+D')}{2}. \tag{29}$$

E. Numerical Testing of the Program for Coupling Versus Separation Distance

The computer program was tested by first applying it to a transmitting circular aperture antenna with a uniform aperture electric field polarized in the x-direction, and a "virtual"[10] receiving antenna inserted in order to compute fields instead of coupling. The on-axis (i.e., mainbeam axis) E_x field of the hypothetical transmitting antenna can be determined analytically and is given by the simple expression

$$E_x(d) = -E_0\left(\frac{d}{\sqrt{d^2+a^2}}\, e^{ik\sqrt{d^2+a^2}} - e^{ikd}\right), \tag{30}$$

with "a" denoting the radius of the circular aperture and E_0 the x-directed aperture electric field. A typical comparison between the on-axis E_x field computed by the program and the exact expression (30) is shown in Fig. 9 for an antenna 20 λ in diameter. Excellent agreement is exhibited throughout the Fresnel region (from $d \approx a$ to $2a^2/\lambda$). For a 100 λ antenna, the program exhibited the same excellent agreement between computed and exact on-axis fields, and took 30 s to compute the on-axis field throughout the Fresnel region on a CDC 6600.

The on-axis fields of these hypothetical antennas vary much more rapidly than most, if not all, existing antennas of the same electrical size. It should also be pointed out that the computer program made no use of the circular symmetry of the hypothetical circular antennas. If this symmetry were utilized the computer run times could be reduced drastically for on-axis fields. However, actual antennas used in practice do not, in general, display this high degree of symmetry. Also, for computations along a radial line other than the mainbeam axis, the strong symmetry of these hypothetical circular antennas with respect to the radial line disappears. (As an example of "off-axis" computation, Fig. 10 shows the magnitude of the E_x field for the same 20 λ antenna of Fig. 9 along a radius making a 30° angle with the mainbeam axis.)

A typical plot of the spherical modal coefficients B_n versus n is shown in Fig. 11 for the on-axis fields of the 20 λ hypothetical circular aperture antenna in Fig. 9. As predicted by the theory [33], [34] discussed in Section III-D, the values of B_n become negligible for $n > N \approx k(a + \lambda)$. (The size a' of the virtual receiving antenna is ignored when computing fields.)

It was mentioned in the introduction that the computer program can also be used to predict near-field gain-correction factors for two antennas. Fig. 12 shows the magnitude of the coupling quotient versus separation distance for two 50 λ diameter circular aperture antennas facing each other, and each with uniform aperture fields polarized in the x-direction. This program took 36 s to compute the coupling quotient on a CDC 6600 throughout the Fresnel region from ($d \approx a + a'$ to $2(a + a')^2/\lambda$). To display the coupling quotient over the entire Fresnel region on a linear scale, the plot in Fig. 12 in the very near field is compressed. An expanded scale, however, shows close agreement between the maximum value of coupling previously shown in Fig. 5 for these same two antennas computed from the program discussed in Section II and the value in Fig. 12 for $d = 50\ \lambda$. Fig. 13 further confirms the theory of Section III-D that the spherical mode coefficients B_n become negligible for $n > N \approx k(a + a' + \lambda)$. Finally, Fig. 14 shows the gain-reduction factor computed between a linearly polarized uniformly illuminated rectangular-aperture antenna and a dipole probe. The dots in Fig. 14 were determined from a direct integration of the aperture field and can be considered exact to within the thickness of the dots.

IV. CONCLUDING REMARKS

We have presented the theory, explained the techniques, detailed the important equations, and described two computer programs for calculating efficiently the mutual coupling at a single frequency between any two antennas arbitrarily oriented and separated in free space. Both programs emphasize efficiency and generality, and require, basically, the complex electric far field of each antenna at a given frequency, and the Eulerian angles designating the relative orientation of each antenna. Multiple reflections between the antennas are neglected but no other restrictive assumptions are involved. If the receiving antenna is nonreciprocal, its complex receiving pattern is required instead of its far field. If an electric field component is desired instead of coupling, the receiving antenna is replaced by a virtual antenna with uniform far field.

The first computer program is based on a plane-wave spectrum approach and uses an FFT algorithm to compute coupling (or fields) versus transverse displacement of the antennas in a plane normal to their axis of separation. An efficient program was made possible by showing that in most cases the spectrum integration need cover only about the solid angle mutually subtended by the smallest spheres circumscribing the antennas. Limiting the integration to this solid angle artificially bandlimits the coupling function thereby allowing much larger integration increments and reducing run times and storage requirements to a feasible amount.

The second program is based on a spherical wave representation of the coupling function and rapidly computes coupling (or fields) versus separation distance between the

[10] A virtual receiving antenna used to compute the x, y, or z-component of electric field of the transmitting antenna is defined by essentially letting the far field $\mathbf{f}'$ of the receiving antenna equal $\hat{e}_{x'}$, $\hat{e}_{y'}$ or $\hat{e}_{z'}$, respectively.

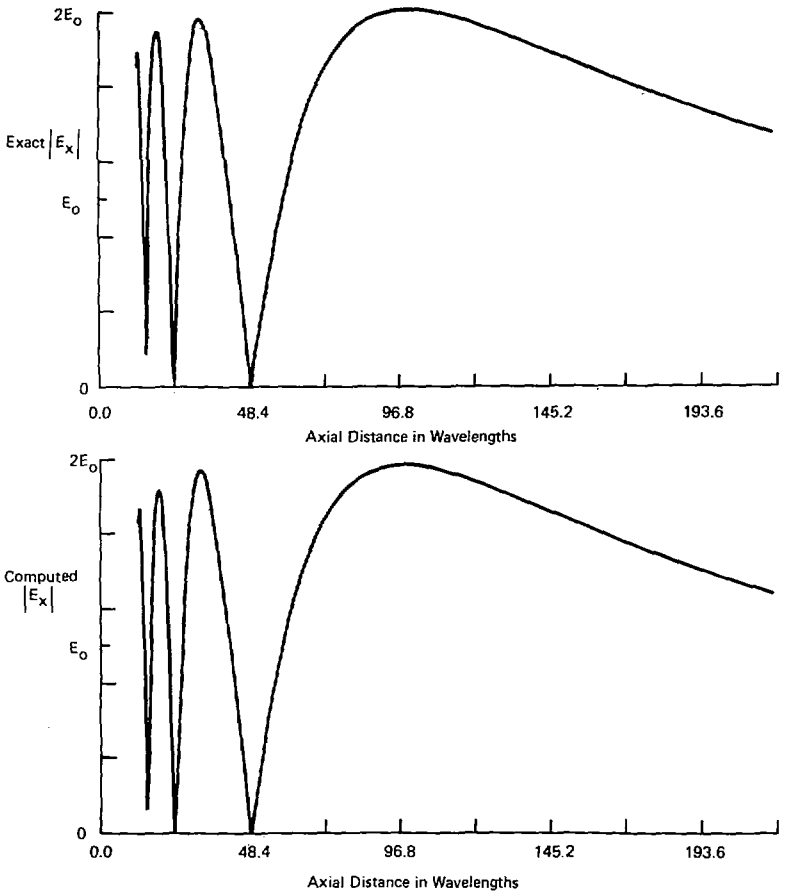

Fig. 9. Computed and exact on-axis electric field for uniform circular aperture antenna 20 λ in diameter.

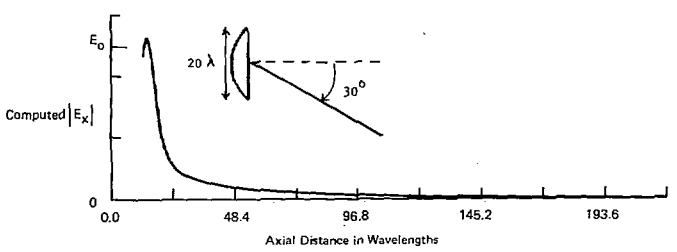

Fig. 10. Computed electric field along 30° axis for uniform circular aperture antenna 20 λ in diameter.

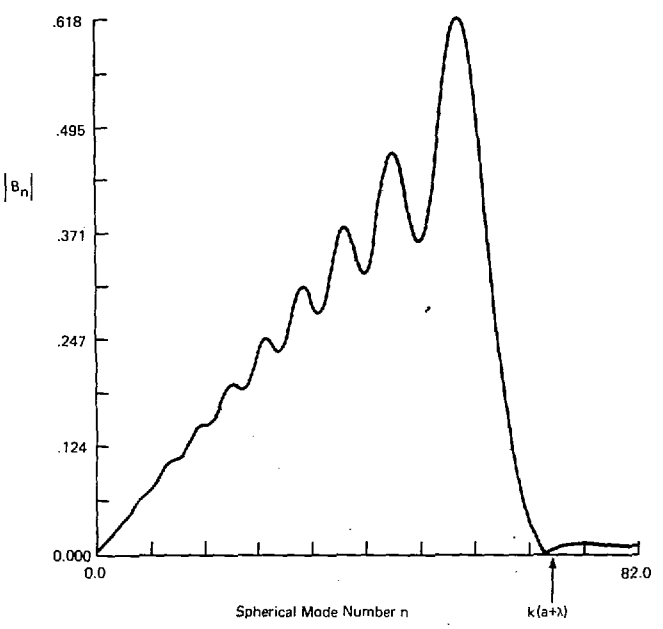

Fig. 11. Plot of magnitude of spherical modal coefficients B_n for the on-axis fields of the 20 λ circular antenna of Fig. 9.

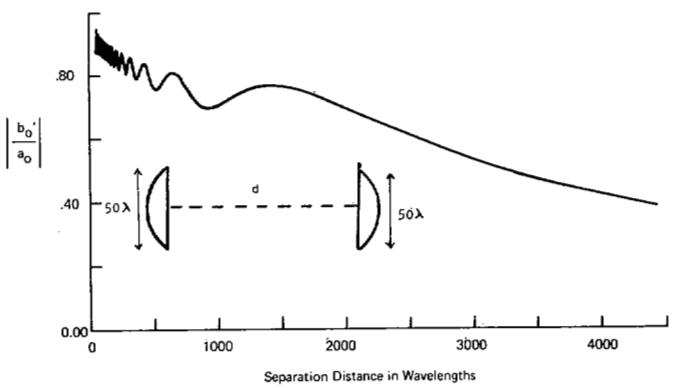

Fig. 12. Magnitude of coupling quotient versus separation distance for two 50 λ circular antennas facing each other.

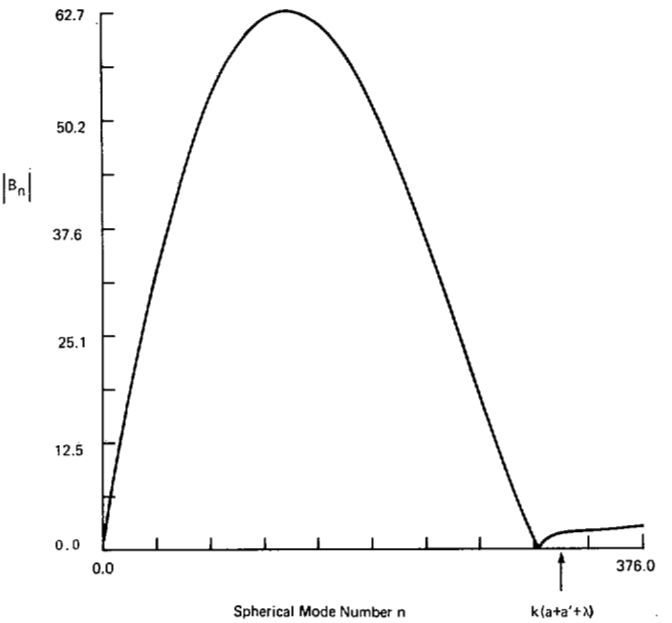

Fig. 13. Plot of magnitude of spherical modal coefficients B_n for the two 50 λ antennas of Fig. 12.

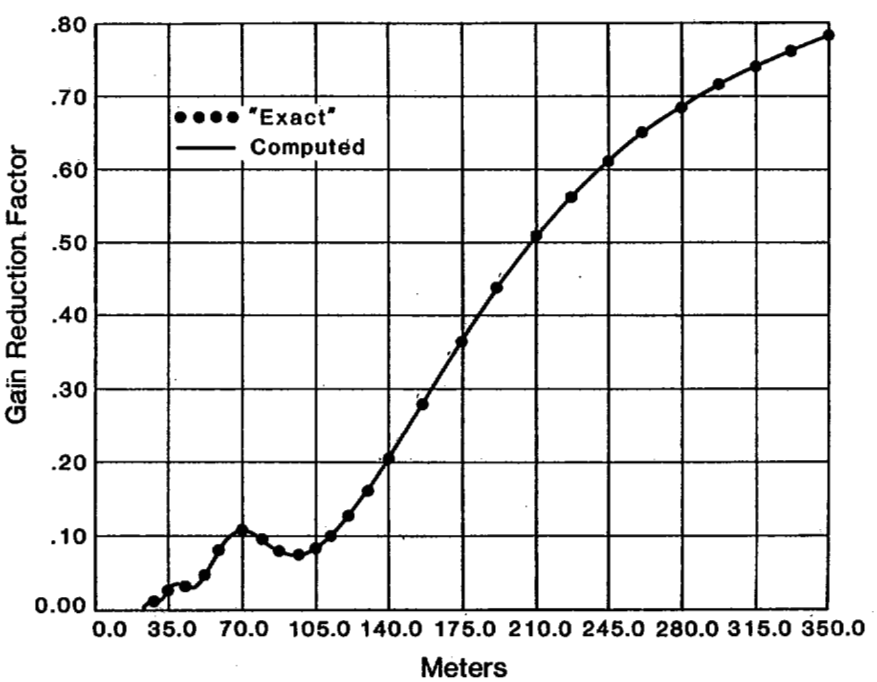

Fig. 14. Gain reduction factor for uniformly illuminated rectangular aperture antenna (55.5 λ × 23.8 λ at 1.3 GHz).

antennas. The spherical wave representation emerged naturally from an intriguing characteristic proven for the mutual coupling function; it, like each rectangular component of electric or magnetic field in free space and like the mutual power spectrum of partial coherence theory, satisfies the homogeneous scalar wave equation. Both programs produce coupling or field values to an accuracy commensurate with the accuracy of the inputted far fields, neglecting multiple reflections.

To compute the coupling of two arbitrary antennas whose diameters sum to 100 λ, or to compute the fields of a single antenna 100 λ in diameter, both programs take about a minute of computer time within core on a CDC 6600. This time is especially noteworthy for the second computer program which computes the coupling quotient along any radial axis throughout the Fresnel region. Also, the first program takes less time for separation distances larger than the sum of the antenna diameters.

One can determine the dependence of computer time and storage upon dimension-to-wavelength ratio of the antennas by looking at (12a) for the first program and (18), (25), and (26) for the second program.

The predominant computation time required by the first program in the evaluation of (12a) for two orthogonal cuts is contributed by the collapsing of the data. For each cut, $2L$ terms are summed $2M$ times resulting in a computer time for electrically large antennas proportional to LM or

$$\left(\frac{D+D'}{\lambda}\right)^2, \tag{31}$$

for a separation distance on the order of $(D + D')$, i.e., in the very near field.

The two FFT's used in the collapsed data evaluation of (12a) require computer storage proportional only to L and M, i.e., proportional to

$$\frac{D+D'}{\lambda}, \tag{32}$$

again for separation distances in the very near field of electrically large antennas. (For larger separation distances these computer storage and time requirements for this first program are diminished by the ratio $(D + D')/d$ and the square of this ratio, respectively.)

The second program also takes computer time and storage proportional to (31) and (32), respectively. Equation (25) sums L terms P times; (26) sums P terms N times and takes N recursions to compute the required N Legendre polynomials for each of the P arguments; (18) sums N terms N_d times for coupling throughout the Fresnel region, and also takes N recursions to compute the required N spherical Hankel functions for each of the N_d arguments. Thus computer time for the second program becomes proportional to $LP + 2NP + 2NN_d$, or proportional to (31) since Section III-D showed that each of these integers, L, N, N_d, and P, become proportional to $(D' + D')/\lambda$ for electrically large antennas. The major in-core computer memory requirements of the second program are for storing the N coefficients B_n, the N spherical Hankel functions and Legendre polynomials, and the P elements of $F(\theta_{0p})$ again amounting to a required computer storage proportional to the ratio (32).

Some qualification to the stated computer times should be made for antennas which have their far fields stored numerically in an external file. In such cases a subroutine must be supplied to retrieve the far fields from the external file and this retrieval plus rollout time can add significantly to the total turn-around time, depending on the accessibility of the file and the efficiency of the retrieval subroutine. Also with some antennas for which coupling of Fresnel-region fields are desired, aperture fields are more readily available or easier to estimate than the far fields. In such cases efficient FFT programs [37], [38] can be applied to the aperture fields to compute the far fields which can then be supplied to the present computer programs.

Finally, although little effort has been devoted to date to compare directly measured and computed values of coupling, the few preliminary comparisons which have been made show agreement to within the experimental limits of error [24], [25].

APPENDIX
EULERIAN ANGLE TRANSFORMATIONS

The basic transformation for the left antenna required to evaluate (8) or (22) explicitly expresses the $x - y - z$ rectangular components of the vector $\mathbf{f}$ in terms of the given $x_A - y_A - z_A$ components and Eulerian angles (ϕ, θ, ψ). Specifically,

$$\begin{bmatrix} f_x \\ f_y \\ f_z \end{bmatrix} = \begin{bmatrix} (\cos\phi\cos\theta\cos\psi - \sin\phi\sin\psi) & (\sin\phi\cos\theta\cos\psi + \cos\phi\sin\psi) & (-\sin\theta\cos\psi) \\ (-\cos\phi\cos\theta\sin\psi - \sin\phi\cos\psi) & (-\sin\phi\cos\theta\sin\psi + \cos\phi\cos\psi) & (\sin\theta\sin\psi) \\ (\cos\phi\sin\theta) & (\sin\phi\sin\theta) & (\cos\theta) \end{bmatrix} \begin{bmatrix} f_{xA} \\ f_{yA} \\ f_{zA} \end{bmatrix} \tag{A1a}$$

or in dyadic notation,

$$\mathbf{f} = \bar{\epsilon} \cdot \mathbf{f}_A. \tag{A1b}$$

The counterpart equation for $(f'_{x'}, f'_{y'}, f'_{z'})$ of the right antenna is the same as (A1) but with (ϕ', θ', ψ') and $(f'_{xp}, f'_{yp}, f'_{zp})$ replacing (ϕ, θ, ψ) and (f_{xA}, f_{yA}, f_{zA}), respectively. It should also be noted that the x, y, and z components of the far field are not independent because there is no radial component of far field. Using $\mathbf{f}_A$, for an example, the rectangular components are related by $\cos\phi_A \sin\theta_A f_{xA} + \sin\phi_A \sin\theta_A f_{yA} + \cos\theta_A f_{zA} = 0$.

The far-field dot product, $\mathbf{f}' \cdot \mathbf{f} = -f'_{x'} f_x + f'_{y'} f_y - f'_{z'} f_z$, is found directly from (A1) and its counterpart equation for the right antenna. The spherical angles (ϕ_A, θ_A) and (ϕ_p, θ_p) in which the far fields of the left and right antennas are given can also be determined from (A1) and its counterpart through the relations

$$k\cos\begin{bmatrix} \theta_a \\ \theta_p \end{bmatrix} = \begin{bmatrix} \mathbf{k} \cdot \bar{\epsilon} \cdot \hat{e}_{zA} \\ \mathbf{k}' \cdot \bar{\epsilon}' \cdot \hat{e}_{zp} \end{bmatrix} \tag{A2a}$$

and

$$\tan\begin{bmatrix} \phi_A \\ \phi_C \end{bmatrix} = \begin{bmatrix} \mathbf{k} \cdot \bar{\epsilon} \cdot \hat{e}_{yA} / \mathbf{k} \cdot \bar{\epsilon} \cdot \hat{e}_{xA} \\ \mathbf{k}' \cdot \epsilon' \cdot \hat{e}_{yp} / \mathbf{k}' \cdot \bar{\epsilon}' \cdot \hat{e}_{xp} \end{bmatrix}. \tag{A2b}$$

One other set of transformations often proves useful. Often, the far field of an antenna is given not in terms of rec-

tangular components but in terms of spherical components. If the electric far-field pattern of the left antenna of Fig. 1 is known in terms of $(f_{\phi A}, f_{\theta A})$, then the rectangular components are related to these spherical components by the spherical angles:

$$\begin{bmatrix} f_{xA} \\ f_{yA} \\ f_{zA} \end{bmatrix} = \begin{bmatrix} -\sin\phi_A & \cos\theta_A \cos\phi_A \\ \cos\phi_A & \cos\theta_A \sin\phi_A \\ 0 & -\sin\theta_A \end{bmatrix} \begin{bmatrix} f_{\phi A} \\ f_{\theta A} \end{bmatrix}. \tag{A3}$$

The counterpart equation for the right antenna giving $(f'_{xp}, f'_{yp}, f'_{zp})$ as functions of $(f'_{\phi p}, f'_{\theta p})$ is formed from (A3) merely by replacing (ϕ_A, θ_A) in the matrix with (ϕ_p, θ_p).

These transformations (A1), (A2), and (A3) must be done for each (k_x, k_y) within the limits of integration needed to evaluate (8) or (22). They look rather cumbersome at first sight, yet computationally they are quite manageable because they involve only sines and cosines of the Eulerian angles and linear dependence upon k_x, k_y, and γ (which equals $\sqrt{k^2 - (k_x^2 + k_y^2)}$). The computer program merely contains subroutines which yield (ϕ_A, θ_A) and (ϕ_p, θ_p) from (A2) and $\mathbf{f}'\cdot\mathbf{f}$ from (A1) and (A3) given the Eulerian angles (ϕ, θ, ψ), (ϕ', θ', ψ'), the integration variables (k_x, k_y), and of course, the far fields $\mathbf{f}_A$ and $\mathbf{f}_C$'

ACKNOWLEDGMENT

Carl F. Stubenrauch of NBS played a major role in the development of the "transverse" computer program. Richard L. Lewis of NBS applied the "longitudinal" computer program to far fields of rectangular aperture distributions to obtain Fig. 14. A technical review by Ronald C. Wittmann of NBS led to a number of simplifications in the presentation of the theory. Discussions with Flemming H. Larsen of the Technical University of Denmark clarified the application of the sampling theorem to Legendre polynominals. The encouragement and support of Hugh C. Maddocks of IITRE, Jacqueline R. Janoski of ECAC, and Ramilan Suwarno of Ft. Huachuca is greatly appreciated.

REFERENCES

[1] D. M. Kerns, "Analytical techniques for the correction of near-field antenna measurements made with an arbitrary but known measuring antenna," URSI-IRE Meeting, Washington, DC, Apr. 29–May 2, 1963.

[2] ——, "Plane-wave scattering-matrix theory of antennas and antenna-antenna interactions," Nat. Bur. Stand. Monograph 162, June 1981.

[3] J. Brown and E. V. Jull, "The prediction of aerial radiation patterns from near-field measurements," *Proc. IEE*, vol. 108B, pp. 635–644, Nov. 1961.

[4] D. M. Kerns, "Correction of near-field antenna measurements made with an arbitrary but known measuring antenna," *Electron. Lett.*, vol. 6, pp. 346–347, May 1970.

[5] R. C. Baird *et al.*, "Recent experimental results in near-field antenna measurements," *Electron. Lett.*, vol. 6, pp. 349–351, May 1970.

[6] A. C. Newell and D. M. Kerns, "Determination of both polarization and power gain of antennas by a generalized 3-antenna measurement method," *Electron. Lett.*, vol. 7, pp. 68–70, Feb. 1971.

[7] D. M. Kerns, "Plane-wave scattering-matrix theory of antennas and antenna-antenna interactions: Formulation and applications," *J. Res. Nat. Bur. Stand.*, vol. 80B, pp. 5–51, Jan.-Mar. 1976.

[8] F. Jensen, "Electromagnetic near-field far-field correlations," Ph.D. dissertation, Tech. Univ. Denmark, Lyngby, 1970.

[9] E. B. Joy and D. T. Paris, "Spatial sampling and filtering in near-field measurements," *IEEE Trans. Antennas Propagat.*, vol. AP-20, pp. 253–261, May 1972.

[10] W. M. Leach, Jr. and D. T. Paris, "Probe compensated near-field measurements on a cylinder," *IEEE Trans. Antennas Propagat.*, vol. AP-21, pp. 435–445, July 1973.

[11] P. F. Wacker, "Non-planar near-field measurements: spherical scanning," Nat. Bur. Stand. Rep. NBSIR 75-809, June 1975.

[12] A. D. Yaghjian, "Upper-bound errors in far-field antenna parameters determined from planar near-field measurements, Part 1: Analysis," Nat. Bur. Stand. Tech. Note 667, Oct. 1975.

[13] ——, "Near-field antenna measurements on a cylindrical surface: A source scattering-matrix formulation," Nat. Bur. Stand. Tech. Note 696, Sept. 1977.

[14] F. H. Larsen, "Probe correction of spherical near-field measurements." *Electron. Lett.*, vol. 13, pp. 393–395, July 1977.

[15] G. V. Borgiotti, "Integral equation formulation for probe corrected far-field reconstruction from measurements on a cylinder," *IEEE Trans. Antennas Propagat.*, vol. AP-26, pp. 572–578, July 1978.

[16] Y. Rahmat-Samii, V. Galindo-Israel, and R. Mittra, " A plane-polar approach for far-field construction from near-field measurements," *IEEE Trans. Antennas and Propagat.*, vol. AP-28, pp. 216–230, Mar. 1980.

[17] W. V. T. Rusch, "Reflector antennas," in *Numerical and Asymptotic Techniques in Electromagnetics*, R. Mittra, Ed. New York: Springer-Verlag, 1975, ch. 7.

[18] R. G. Kouyoumjian, "The geometrical theory of diffraction and its application," in *Numerical and Asymptotic Techniques in Electromagnetics*, R. Mittra, Ed. New York: Springer-Verlag, 1975, ch. 6.

[19] J. F. Kauffman, W. F. Croswell, and L. J. Jowers, "Analysis of the radiation patterns of reflector antennas," *IEEE Trans. Antennas Propagat.*, vol. AP-24, pp. 53–65, Jan. 1976.

[20] V. Galindo-Israel and R. Mittra, "A new series representation for the radiation integral with application to reflector antennas," *IEEE Trans. Antennas Propagat.*, vol. AP-25, pp. 631–641, Sept. 1977.

[21] R. C. Rudduck and S. H. Lee, "Numerical electromagnetics code—reflector antenna code, Part I: User's manual, Part II: Code manual," The Ohio State Univ. ElectroSci. Lab., Tech. Rep. 784508-19 and 16, Sept. 1979.

[22] M. K. Hu, "Near-zone transmission formulas," IRE Nat. Conv. Record, vol. 6, pt. 8, pp. 128–138. 1958.

[23] T. S. Chu and R. A. Semplak, "Gain of electromagnetic horns," *Bell System Tech. J.*, vol. 54, pp. 527–537, Mar. 1965.

[24] A. D. Yaghjian and C. F. Stubenrauch, "Efficient computation of coupling between co-sited antennas from the far field of each antenna," in *Digest USNC/URSI Meeting*, Boulder, CO, Nov. 1978, p. 167.

[25] A. D. Yaghjian, "Efficient computation of the mutual coupling between co-sited antennas," NBS Report No. SR-723-55-80, 1980, unpublished.

[26] J. S. Ames and F. D. Murnaghan, *Theoretical Mechanics*. Boston: Ginn, 1929, ch. 2.

[27] W. T. Cathey, *Optical Information Processing and Holography*. New York: Wiley, 1974, ch. 2.

[28] *IEEE Trans. Audio Electroacoustics*, June 1967.

[29] L. J. Kaplan *et al.*, "Rapid measurement and determination of antenna patterns using collapsed near-field data," in *Digest Int. Symp. IEEE AP-S*, Stanford Univ., pp. 370–373, June 1977.

[30] C. C. Johnson, *Field and Wave Electrodynamics*. New York: McGraw-Hill, 1965, sec. 10.5.

[31] J. A. Stratton, *Electromagnetic Theory*. New York: McGraw-Hill, 1941, sec. 7.3.

[32] C. Muller, *Foundations of the Mathematical Theory of Electromagnetic Waves*. New York: Springer-Verlag, 1969, p. 339.

[33] L. J. Chu, "Physical limitations of omni-directional antennas," *J. Appl. Phys.*, vol. 19, pp. 1163–1175, Dec. 1948.

[34] E. B. Ojeba and C. H. Walter, "On the cylindrical and spherical wave spectral content of radiated electromagnetic fields," *IEEE Trans. Antennas Propagat.*, vol. AP-27, pp. 634–639, Sept. 1979.

[35] *Handbook of Mathematical Functions*, Nat. Bur. Stand. Appl. Math. Series-55, M. Abramowitz and I. A. Stegun, Ed. Washington, DC: U.S. Gov. Printing Office, June 1964, ch. 8–10.

[36] R. C. Hansen, *Microwave Scanning Antennas*. New York: Academic, 1964, vol. 1, ch. 1.

[37] A. G. Repjar, "Planar near-field computations (software and results)," Nat. Bur. Stand. Short Course, Antenna Parameter Measurement by Near-Field Techniques, Aug.–Sept. 1977.
[38] R. L. Lewis, "Efficient computation of the far-field radiated by an arbitrary rectangular-aperture distribution," Nat. Bur. Stand. Internal Rep. 81-1643, Mar. 1981.
[39] M. J. Beran and G. B. Parrent, Jr., *Theory of Partial Coherence*. Englewood Cliffs, NJ: Prentice-Hall, 1964, sec. 4.4.
[40] F. H. Larsen, "Spherical near-field transformation program with probe correction," Electromagn. Inst. Rep. 201, Tech. Univ. Denmark, Oct. 1978.

Arthur D. Yaghjian (S'68–M'69) was born in Providence, RI on January 1, 1943. He received the B.S., M.S., and Ph.D. degrees in electrical engineering from Brown University, Providence, RI in 1964, 1966, and 1969.

After teaching mathematics and physics for a year, he joined the Electromagnetics Division of the National Bureau of Standards, Boulder, CO, where his major research has been in near-field antenna measurements, underwater acoustics, and electromagnetic theory.

Adaptive Arrays: A New Approach to the Steady-State Analysis

SHALHAV ZOHAR, SENIOR MEMBER, IEEE

Abstract—**Our main goal is a closed-form expression for the steady-state output signal-to-noise ratio (SNR) of an n-element adaptive array excited by one desired narrow-band signal and $K-1$ narrow-band jammers. This is facilitated by representing each excitation by a complex n-dimensional vector—the excitation vector. We show that the important system parameters are functions of scalar products of pairs of these exctiation vectors. In particular, the normalized output SNR of the array is shown to be the ratio of determinants whose elements involve these scaler products. Such determinants are also shown to be involved in the expressions for the optimal array weights.**

I. INTRODUCTION

THE MAIN function of an adaptive array is to maximize its output signal-to-noise ratio (SNR) in the presence of a time varying configuration of signals and jammers. Our purpose here is to derive a closed-form expression for the steady-state output SNR in a configuration of one signal and an arbitrary number of jammers. Our result is quite general, being valid for an array consisting of an arbitrary (three-dimensional) arrangement of arbitrary antenna elements. We also obtain the optimal weights for such a general type of array. Both these results are expressed as ratios of determinants involving scalar products of the basic system vectors.

Consider an adaptive array consisting of n arbitrary antenna elements operating in an environment of K spatially distinct narrow-band sources. One of these (source number 1) is the desired signal while the remaining $(K-1)$ sources are jammers. The array processor constructs the (single) array output voltage as a linear combination of the n individual antenna voltages. The main challenge here is to choose the (complex) coefficients of this linear combination (known as the weights) in such a way that the jammers will be attenuated with respect to the desired signal. More precisely, the weights are chosen to maximize

$$\gamma = \frac{\text{output signal power}}{\text{output noise power}} \tag{1}$$

where the term "noise power" covers the jammers as well as thermal noise. The solution to this problem has been known for quite some time [1], [4], [6]. In Section III we present a short derivation of this solution which is tailored to our specific requirements. Building on this foundation, we then proceed to obtain the closed-form expression for the SNR.

The main feature distinguishing our approach from earlier work is the base adopted for the representation of the weights vector. Whereas the eigenvectors of the noise covariance matrix adopted in [6], [4] are very suitable for the analysis of the transient behavior of the array, it turns out that the steady-state analysis is much better served by a base consisting of the excitation vectors[1] of the sources exciting the array. We have found that this formulation provides insight which has already shed light on a failure mechanism of adaptive arrays [7] as well as the structure of the adapted beam pattern. Furthermore, this formulation provides the foundation for an improved algorithm for a multiple-access communication system based on adaptive arrays [8].

II. ADOPTED LINEAR-ALGEBRA FORMALISM

In our mathematical manipulations we use dyadics throughout. For the reader who is not familiar with the subject, we provide all the necessary background in Appendix A. At this

Manuscript received April 7, 1980; revised December 18, 1980, March 18, 1981, and July 2, 1981. The research described in this paper was carried out at the Jet Propulsion Laboratory, California Institute of Technology, and was sponsored by the U.S. Army Communications and Electronics Command through an agreement with the National Aeronautics and Space Administration.

The author is with the Jet Propulsion Laboratory, California Institute of Technology, Mail Stop 238-420, 4800 Oak Grove Drive, Pasadena, CA 91109.

[1] Precise definitions are given later.

0018-926X/82/0100-0128$00.75